

**Numerical and Theoretical Investigation of Wheel-Rail Contact**

Ramazan ÖZMEN

*Department of Mechanical Engineering, Karabük University, Karabük, Turkey.*

**Abstract** —The aim of this study is to analyze the dynamic interaction between wheel and rail by finite element method (FEM). The contact parameters through the movement of a wagon wheel on the 60 E1 rail profile is investigated by the dynamic analysis based FEM. The wheel and rail profile are assumed as unworn members. The contacting bodies must be elastic according to Hertz contact theory (HCT). Thus, the material properties of the wheel and rail are defined as elastic for comparing results of finite element analysis with HCT. It was concluded from FEM results that a certain mesh size is sufficient in order to find the contact force, but the mesh size must be reduced to obtain the contact area depending on the Hertz contact theory.

**Keywords**—Rail, Hertz Contact Theory, FEM, Contact Force, Contact Area

**I. INTRODUCTION**

The wheel-rail contact is a crucial situation effecting the reliability of the railway system and vehicle performance and is altered by many factors, i.e. track geometry, vehicle suspension, wheel and rail profiles. The contact theory of Hertz has been broadly implemented in many engineering fields to deal with contact problems [1][2]. The contact area between the wheel rail is exposed to high pressures and shear stresses. This causes the deformation of wheel and rail directly. Damage mechanisms such as surface cracks, plastic deformation and abrasion shorten the service life of the railway and vehicles. Calculation of the contact forces acting on the contact area between the wheel and the rail is a crucial step in determining the dynamic performance of the wheel rail system [3][4].

The studies concerning with the interaction between wheel and rail from several aspects is found in the literature. The solution of the contact problem between wheel and rail according to the methodology applied by Pater [5] includes four subproblems classified as geometric problem, normal problem, kinematic problem and tangential problem. The calculation of the forces between the wheel and the rail, the shape and size of the contact area, and the determination of the pressure distribution in the contact area is defined as normal problem. Yan and Fischer [1] examined the applicability of the Hertz contact theory to the contact problem between wheel and rail for the UIC60 standard rail, Cr 135 crane rail and crossing nose. They investigated not only elastic contact but also elastic-plastic contact. The numerical results were compared only with the Hertz contact theory for the elastic contact problem. It was stated that the results obtained by the numerical solution converged with the Hertz contact theory calculations in the case of regarding the wheel and rail as elastic. Vo et al. [6] investigated the effect of friction on contact stress distribution and material behavior during the contact between the wheel and rail for three different friction conditions by finite element method. They stated that a significant increase in Von-mises stress occurs when the adhesion coefficient is increased. They also specified that high stresses in the shear zone formed on the contact surface cause surface damage such as plastic flow, wear and surface cracks.

Several methods have been used to investigate the wheel-rail contact by many researchers. For example, Pau et al. [7] tried to estimate the contact pressure distribution at the contact region with ultrasonic technique and determined the size and shape of the contact area. They emphasized that the ultrasonic method can be used for investigating the wheel-rail contact parameters due to its simplicity and reliability. Telliskivi and Olofsson [3] investigated the contact between wheel and rail by using measured profiles in the sharp curved track for the two contact cases through employing Finite element method, Hertz method and Kalker's program of Contact. It was concluded that the results of the finite element method do not significantly agree with Hertz's analytical method and Kalker's Contact software for the contact zone in rail corner due to the half-space assumption. Sladkowski and Sitarz [8] investigated the contact zone distributions for different wheelset attack angles via Finite element method. Kubin et al. [9] developed a two-dimensional finite element model including wheel and rails measured surface roughness. They investigated the effects of roughness on the rail surface deformation for a wheel rolling on a rail. It was concluded from their calculations that increasing the traction increases the plastic shear strain on the rail surface and normal load has a small effect on the plastic strain. The other parts of the track are investigated by some researchers. Contact stress distributions for the three joint materials near the insulated rail joints is investigated with the three-dimensional finite element model established by Chen and Kuang [10]. They specified that the insulated rail joints effect the contact stress distribution and Hertz contact theory is impracticable for near insulated rail joints.

In this study, the dynamic behavior of the wagon wheel with S1002 profile on the 60E1 type rail was investigated by dynamic analysis based on finite element method. It was assumed that the wheel and rail profiles were unworn. Since the bodies contacting each other are elastic in the Hertz contact theory, the material of the wheel and rail was defined as

elastic. The contact forces and contact area sizes obtained via numeric analysis were compared with results of the Hertz contact theory calculation.

## II. METHODOLOGY

### A. Hertz Contact Theory

In this study, firstly finite element analysis was done in order to determine the contact parameters (contact force and area) resulting from wheel and rail interaction. Then, the Hertz contact theory is used to verify the results of finite element model.

Hertz published the theory of contact between elastic bodies under the following assumptions in 1881 [6]. Accordingly:

- The material of the contacting objects must be elastic.
- The area of contact is considerably smaller than the radius of the local curvature of the contact areas.
- The radii of curvature are constant within the contact area limits.
- The field of stress in the contacting bodies can be estimated by the area of stress in the semi-infinite space.

The resultant contact area has an elliptical shape and the contact area can be considered straight according to these assumptions. Also, the pressure distribution in the contact zone is semi-ellipsoid form. Based on Hertz contact theory, the normal pressure is distributed in ellipsoid form over the elliptical contact area with a and b half axes. The distribution of the ellipsoidal contact pressure  $p(x, y)$  is calculated by Eq. (1) [7].

$$p(x, y) = \frac{3F}{2\pi ab} \sqrt{1 - \left(\frac{x}{a}\right)^2 - \left(\frac{y}{b}\right)^2} \quad (1)$$

The half-axis lengths of the contact ellipse are defined as:

$$a = m(3\pi F_n(K_1 + K_2)/4K_3)^{1/3} \quad (2)$$

$$b = n(3\pi F_n(K_1 + K_2)/4K_3)^{1/3}$$

Here  $K_1$  and  $K_2$  are constants that depend on material properties and is calculated by Eqns. (3-4):

$$K_1 = \frac{1 - (\nu^i)^2}{\pi E^i}, \quad K_2 = \frac{1 - (\nu^j)^2}{\pi E^j} \quad (3)$$

The value of  $K_3$  presented in equation (2) is given as follows according to the geometrical properties of the contacting bodies.

$$K_3 = \frac{1}{2} \left( \frac{1}{R_1^i} + \frac{1}{R_2^i} + \frac{1}{R_1^j} + \frac{1}{R_2^j} \right) \quad (4)$$

The coefficients of m and n in the formulas given for the half-axis lengths of the contact ellipse are tabulated by Hertz as the function of the angular parameter ( $\theta$ ) varying from  $0^\circ$  to  $180^\circ$  and are defined as follows:

$$\theta = \cos^{-1}(K_4/K_3) \quad (5)$$

The value of  $K_4$  presented above is derived from the equation (5) and is calculated by Eq. (6).

$$K_4 = \frac{1}{2} \sqrt{\left(\frac{1}{R_1^i} - \frac{1}{R_2^i}\right)^2 + \left(\frac{1}{R_1^j} - \frac{1}{R_2^j}\right)^2 + 2\left(\frac{1}{R_1^i} - \frac{1}{R_2^i}\right)\left(\frac{1}{R_1^j} - \frac{1}{R_2^j}\right)\cos\Psi} \quad (6)$$

The coefficients of m and n corresponding to the ( $\theta$ ) value can be calculated by performing a linear or cubic interpolation [7]. It can also be found by applying closed form solution as a function of m and n values.

### B. Finite Element Model

Elasticity of the ground is one of the most crucial factors affecting the dynamics of the vehicle in railway track systems. Different assumptions have been used in the literature to identify the elasticity of the ground. The sleepers modeled under the rails and bending of the rails among the sleepers is considered [11]. Also, the movement of the rail in the vertical direction is assumed to be zero by defining the rail base contacting with a rigid ground [12]. In this study, the method used by Pletz et al. [13] was taken as reference for defining the ground properties contacting with base of the rail. Instead of a complex damping system, the rail base is connected rigidly to a suspension system using a simple spring and damper element. Since the entire base of the rail is connected to the suspension system, the bending of the rail between the sleepers is neglected. In the described suspension system, the spring and damping coefficients were taken as  $k_t=90$  kN/mm and  $c_t=250$  kNs/m respectively. Furthermore, to represent the primary suspension system of the bogie, the

movement of the wheel in the vertical direction was controlled by a damping element with a coefficient of 53 kNs / m. The coefficient of friction between the wheel and the rail was taken as 0.3. Hertz contact theory assumes that the contacting bodies touching together are elastic. In order to compare the results between the finite element analysis and Hertz calculations, the wheel and rail were assumed to be elastic and the defined material coefficients are given in Table 1.

Table1 Material Properties		
Young`s Modulus[GPa]	Poisson`s Ratio	Density [kg/m <sup>3</sup> ]
210	0.3	7850

Some simplifications and limitations were made in the analysis to reduce the calculation time. The movement freedom of the wheel in the lateral direction was restricted. Similarly, the rolling and yawing movement of the wheel was neglected for the analyzed section, and the freedom of rotation in the vertical direction of the wheel and in the direction of the running line is also restricted. In order to shorten the calculation time, the mesh size in the contact region was made finer than the other regions. The "tie constraint" command in the ABAQUS software was used to connect rough and fine meshed regions.

In this study, the dynamic interaction between the wagon wheel and the rail was investigated by using finite element software of ABAQUS / Explicit. The three-dimensional model is consisted of single wheel and 2 m long rail. The wheel has a profile of S1002 with 0.46m diameter. The axle of the wheel is considered to be rigid. The UIC 60 E1 type rail was used and inclined by 1/40 slope corresponding to the cant angle of 1.432°. In the study, the movement of the wheel was evaluated by the dynamic analysis method with 79.7 kN axle load at a speed of 100 km/h. The variation of contact forces between the wheel and rail and the formation of contact area was investigated by the three-dimensional finite element model. The contact area was modeled as two different mesh sizes in order to realize the variation of contact force between the wheel and the rail. The rail was modeled as two parts and approximately 120750 number of C3D8R type 8-node linear cubic elements were used. The wheel was modeled as three parts and the tread of the wheel forming the contact area was meshed with an element dimension of 2.9mm and consists of about 14000 elements totally.

### III. RESULTS and DISCUSSION

The wheel is travelled approximately 2 m distance on the rail in finite element analysis. The variation of contact force with the running of wheel on rail under the axle load of 80 kN and a wheel speed of 100 km/ h is given in Figure 1. In Figure 1, the big contact force oscillations were seen at the beginning of the analysis due to the first contact of the wheel to the rail. The large oscillations that seen initially were damped with the vertical damping element defined at the wheel center, and the oscillation of contact force is maintained near the applied axle load after about 400 mm of wheel movement.

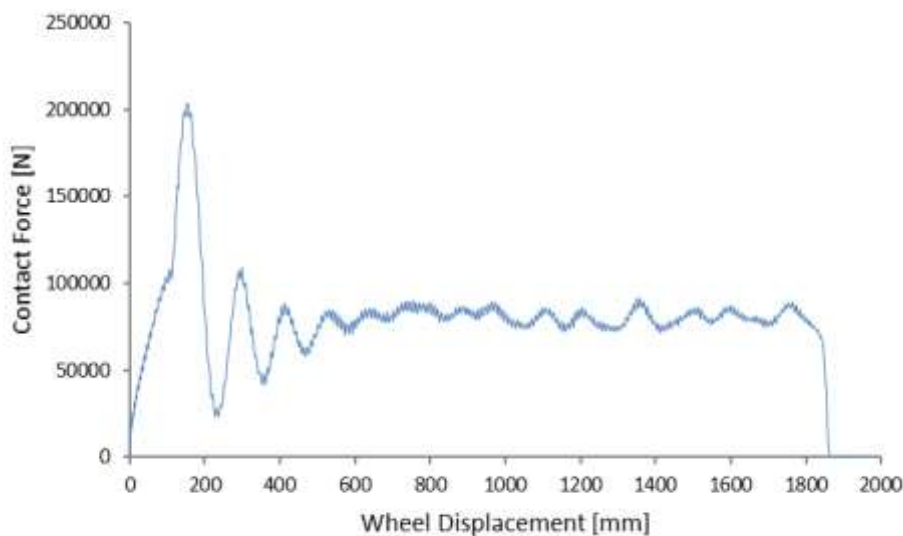


Figure 1. Vertical contact forces between wheel and rail (Mesh size of 2.8mm)

At the beginning of the study, the mesh size was applied as 2.8 mm in the regions where the wheel and rail contact each other. When the formation of the contact area obtained from the analysis was examined, it was seen that the contact area size was much higher than calculated by Hertz contact theory. Numerous sizes of mesh were examined the influence of mesh size on the contact area size. For this reason, the mesh size is reduced from 2.8 mm to 1.8 mm. The resulting

change in contact area is given in Figure 2. According to the Figure 2, as the mesh size of the model decreases, it was seen that the obtained contact area also decreases.

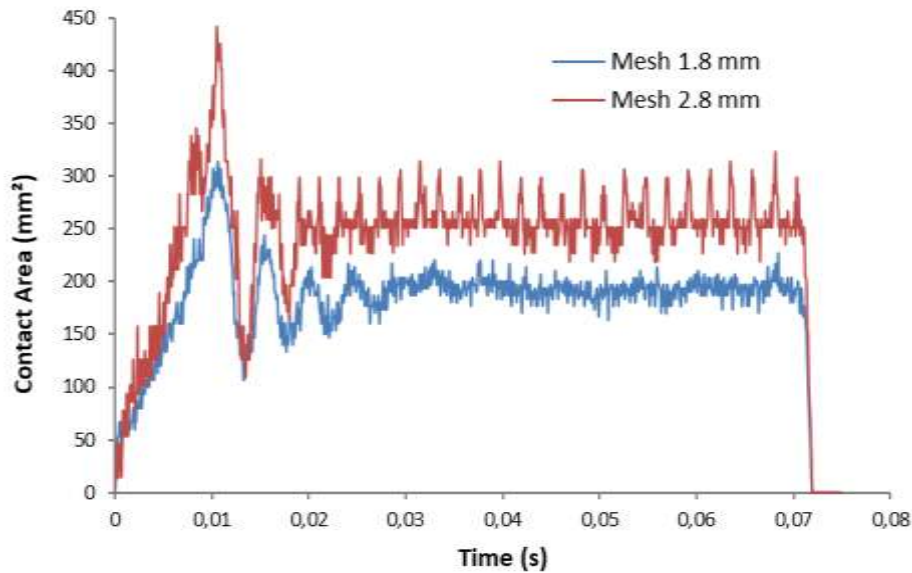


Figure2. Thevariation of contactarea

In order to investigate the influence of the mesh size on the contact force, the variation of the contact force depending on the mesh size was also investigated. The change in contact force between the wheel and rail for both mesh sizes is given in Figure 3.

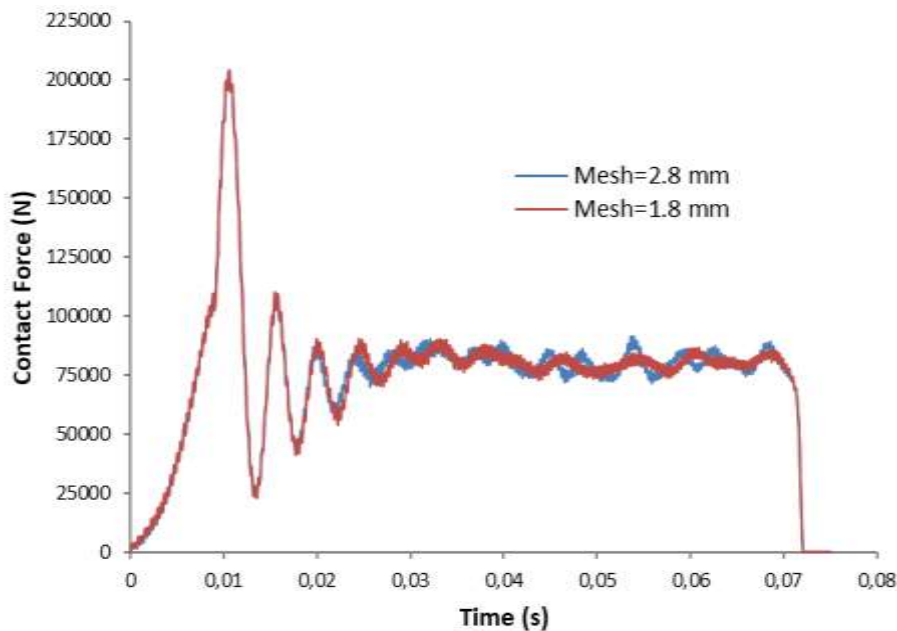


Figure3. Comparison of verticalcontactforcesfordifferent mesh sizes

It can be seen from Figure 3 that the high contact force oscillations originated at the beginning of the simulation are same for both mesh sizes. The range of oscillations in the contact force at the later stages of the simulation are seen to decrease as the mesh size decreases. When the effect of the mesh sizes on contact area are evaluated, the obtained contact area converged to the calculated value by Hertz theory with decreasing the mesh size. In this context, a mesh size of 1 mm and 0.3 mm was tried to approach the magnitude of contact area calculated by Hertz contact theory. The average contact area for a 1 mm mesh size from the FEM simulation was obtained as 165 mm<sup>2</sup>. The magnitude of the contact area calculated by the Hertz contact theory with respect to the defined wheel-rail parameters and axle load used in the analysis is 120 mm<sup>2</sup>. As the mesh size decreases, the lengths of examined regions are also shortened because of the increase in the number of elements used in the FEM model. As the mesh size is decreased in the model, the stable time increment decreases over time in the software. This leads to an increase in the analysis time required to complete the solution due to increase in the number of increments. Figure 4 shows the examined finite element model (region A) for the mesh size of 0.3 mm. Additionally, the region examined for the contact area change is located close to the region where the

oscillations decrease in contact force because of the increase in the analysis time in the use of low mesh sizes. This allows the analysis to be completed in a shorter time for low mesh sizes.

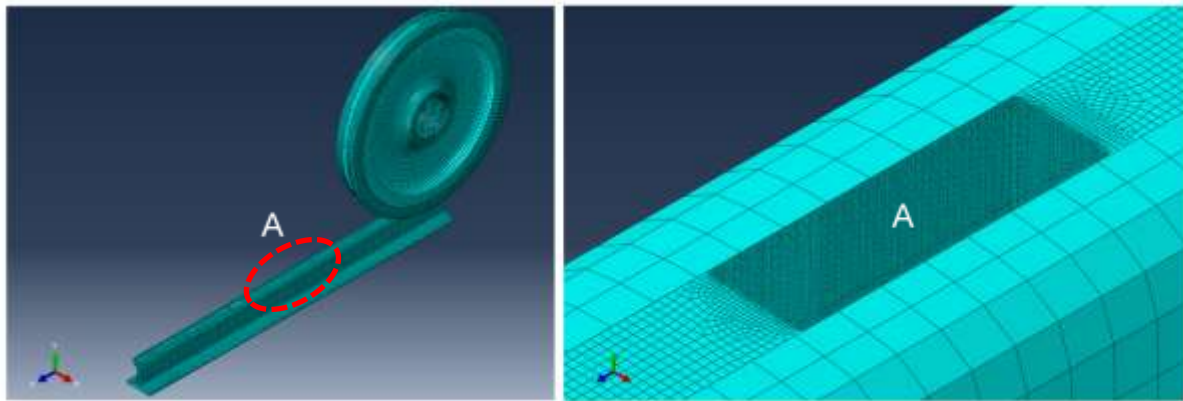


Figure 4 Finite element model and investigated section for the 0.3 mm mesh size

The variation of the contact areas obtained from the analyses and calculated with Hertz contact theory is given in Figure 5.

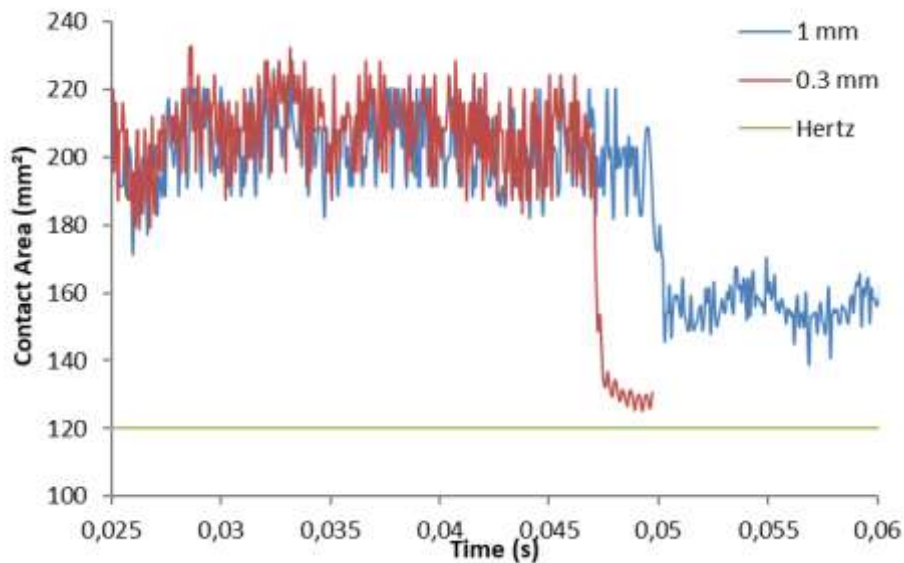


Figure 5 Comparison of obtained contact areas with calculated Hertz contact theory

When the analysis results of 1 mm and 0.3 mm mesh size regions are compared, as the mesh size of the contact regions decreases the magnitude of the contact area. As can be seen from Fig. 5, the contact area was obtained larger for the bigger mesh size at the beginning of the analysis while the contact area was obtained close to the Hertz contact theory when it was moved to finer mesh region (seen A). The contact area sizes obtained as a result of the analysis are given in Table 2. The average contact area for a 0.3 mm mesh size was obtained as 130 mm<sup>2</sup>. In this case, the differences of contact areas between the calculated from Hertz theory and obtained from analysis was found to be 7.69%.

The results show that the convenient results with theoretical approaches will be obtained when lower mesh size is used. In addition, this modeling approach can be used to predict the damage that may occur due to wheel-rail interactions in real conditions.

Table 2 Change in the contact area according to mesh size		
Mesh size (mm)	Contact area (mm <sup>2</sup> )	Difference (%)
Hertz	120	-
1	165	27.7
0.3	130	7.69

#### IV. CONCLUSION

This study focused on the variation of the contact force and contact area between the wheel and rail depending on the mesh size by using finite element method. Also, the obtained results by FEM were compared with the Hertz contact theory, and the overall results are summarized as follows:



1. When the effect of the mesh size on wheel-rail interactions was examined, the oscillations originating from the mesh size decreased and the contact force at the lower mesh dimensions became more stable.
2. According to the analysis results, the magnitude of the contact area closed to the calculated value by Hertz contact theory when the mesh size of the contact areas was decreased. As a result of mesh size application of 0.3 mm, it was seen that there was a difference of 7.69% compared with to the contact area calculated by Hertz contact theory.
3. The closeness of the obtained results by finite element analysis to the Hertz contact theory shown the suitability of the developed finite element model. Therefore, the damages occurred in wheel-rail interaction such as wear, crack, etc. can be predicted by using this modeling approach.

## REFERENCES

- [1] W. Yan and F. D. Fischer, "Applicability of the Hertz contact theory to rail-wheel contact problems," *Arch. Appl. Mech. (Ingenieur Arch.)*, vol. 70, no. 4, pp. 255–268, 2000.
- [2] C. Barbinta, C. Ulianov, F. Franklin, and S. Cretu, "Wheel-rail contact modelling and analysis , considering profiles types and lateral displacement," in *TRA2014 Transport Research Arena*, 2014.
- [3] T. Telliskivi and U. Olofsson, "Contact mechanics analysis of measured wheel – rail," *Proc. Inst. Mech. Eng. Part F- J. Rail Rapid Transit*, vol. 215, pp. 65–73, 2001.
- [4] M. Toumi, H. Chollet, and H. Yin, "Finite element analysis of the frictional wheel-rail rolling contact using explicit and implicit methods," *Wear*, pp. 1–10, 2016.
- [5] N. Bosso, M. Spiryagin, A. Gugliotta, and A. Somà, "*Mechatronic Modeling of Real-Time Wheel-Rail Contact.*" Springer Berlin, 2013.
- [6] K. D. Vo, A. K. Tieu, H. T. Zhu, and P. B. Kosasih, "A 3D dynamic model to investigate wheel – rail contact under high and low adhesion," *International Journal of Mechanical Sciences* vol. 85, pp. 63–75, 2014.
- [7] M. Pau, "Estimation of real contact area in a wheel-rail system by means of ultrasonic waves," *Tribol. Int.*, vol. 36, no. 9, pp. 687–690, 2003.
- [8] A. Sladkowski and M. Sitarz, "Analysis of wheel – rail interaction using FE software," vol. 258, no. March 2004, pp. 1217–1223, 2005.
- [9] W. K. Kubin, M. Pletz, W. Daves, and S. Scheriau, "A new roughness parameter to evaluate the near-surface deformation in dry rolling / sliding contact," *Tribology Int.*, vol. 67, pp. 132–139, 2013.
- [10] Y. C. Chen and J. H. Kuang, "Contact stress variations near the insulated rail joints," *Proceedings of the Institution of Mechanical Engineers , Part F : Journal of Rail and Rapid Transit* 2002.
- [11] X. Zhao, Z. Wen, M. Zhu, and X. Jin, "A study on high-speed rolling contact between a wheel and a contaminated rail," *Veh. Syst. Dyn.*, vol. 52, no. 10, pp. 1270–1287, 2014.
- [12] X. Zhao and Z. Li, "The solution of frictional wheel-rail rolling contact with a 3D transient finite element model: Validation and error analysis," *Wear*, vol. 271, no. 1–2, pp. 444–452, 2011.
- [13] M. Pletz, W. Daves, and H. Ossberger, "A wheel passing a crossing nose: Dynamic analysis under high axle loads using finite element modelling," *Proc. Inst. Mech. Eng. Part F J. Rail Rapid Transit*, vol. 226, no. 6, pp. 603–611, 2012.